

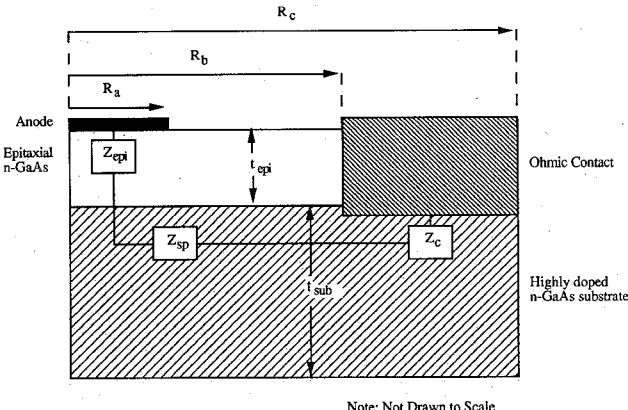
# Series Impedance of GaAs Planar Schottky Diodes Operated to 500 GHz

Kaushik Bhaumik, Boris Gelmont, Robert J. Mattauch, *Fellow, IEEE*, and Michael Shur, *Fellow, IEEE*

**Abstract**—This paper discusses the impact of ohmic contacts on the series impedance of a GaAs cylindrical planar Schottky diode. The expression for the high-frequency impedance of an annular ohmic contact is developed using a novel transmission line model. This formulation is used to ascertain the contribution of the ohmic contact impedance to the overall device series impedance at both dc and 500 GHz. Diode impedance characterization indicates that the ohmic contact impedance makes a small contribution to the series impedance in comparison to that of the other components, both at dc and submillimeter wavelengths. Hence, the dimensions of the contact pads can be scaled down significantly without any appreciable increase in series impedance but with a decrease in the parasitic pad-to-pad capacitance. Finally, this modeling establishes theoretical guidelines regarding the allowable limits for specific contact resistance in small geometry diodes, so that device *I*-*V* characteristics are not significantly altered as a result of the ohmic contact impedance.

## I. INTRODUCTION

GaAs Schottky diodes are used as signal mixers and varactor elements in radio astronomy, atmospheric physics and plasma diagnostics applications up to the terahertz frequency range. The traditional whisker-contacted diode suffers from an inherent mechanical instability and inductance which make it unsuitable for use in harsh mechanical environments, such as those encountered in space-based radiometry. The planar Schottky diode was developed to overcome these shortcomings and to promote diode integration into MMIC's. Unfortunately, state-of-the-art GaAs planar diodes have achieved efficient signal mixing capability only up to 300 GHz [1]. This limit is due in part to parasitics such as shunt and series capacitances. To raise this frequency limitation, the diode series impedance must be reduced by means of op-



Note: Not Drawn to Scale

Fig. 1. Geometry of cylindrical planar diode with impedance components.

timized material parameters, device geometry and ohmic contact technology.

This paper assesses the impact of ohmic contacting technology on the electrical characteristics of the cylindrical planar diode through the use of a lumped model (LEM) for the series impedance components, shown in Fig. 1. In developing impedance expressions, we assume that the substrate is heavily doped compared to the active epilayer, such that current flows down from the anode through the epilayer and spreads into the substrate; where it is confined to within a skin depth or by the thickness of the substrate, whichever is smaller, until it reaches the ohmic contact.

In the lumped element model, the series impedance is divided into three components: epitaxial layer impedance ( $Z_{\text{epi}}$ ), bulk spreading impedance at the epilayer/substrate interface ( $Z_{\text{sp}}$ ) and the ohmic contact impedance ( $Z_c$ ). Analytical expressions for the first two components have been derived by other researchers and their results are summarized here. An expression for the dc impedance of an ohmic contact in a cylindrical diode is developed using a circular Transmission Line Model (TLM), similar to the analysis performed by Reeves [2]. This expression is then reformulated, by solving Maxwell's curl equations subject to the circuit conditions posed by the circular TLM, to arrive at a high-frequency impedance expression. The use of both of these expressions provides the device designer a means of characterizing the effect of ohmic contact technology on the device impedance at both dc and operational frequencies.

Manuscript received September 10, 1991; revised December 23, 1991. This work was supported by The National Science Foundation through grant no. ECS-9016063; The Office of Naval Research through grant no. N-0014-90-J-40006 under the direction of Dr. Y. Park; The Army Research Office through grant no. DAAL03-91-G-0048; and The Virginia Center for Innovative Technology.

K. Bhaumik is with the School of Electrical Engineering, Cornell University, Ithaca, NY 14853.

B. Gelmont, R. J. Mattauch and M. Shur are with the Department of Electrical Engineering, University of Virginia, Charlottesville, VA 22903-2442.

IEEE Log Number 9106763.

## II. EPITAXIAL LAYER AND BULK SPREADING IMPEDANCES

The epitaxial layer impedance,  $Z_{\text{epi}}$ , is modeled as being that of a fully undepleted disk of semiconductor material. It is assumed that no spreading occurs within this disk or at the interface with the substrate. As such,  $Z_{\text{epi}}$ , is formulated as

$$Z_{\text{epi}} = \frac{t_{\text{epi}}}{\sigma_{\text{epi}} \pi R_a^2}. \quad (1)$$

The conductivity within the epitaxial layer,  $\sigma_{\text{epi}}$ , is calculated by

$$\sigma_{\text{epi}} = \frac{\sigma_o}{1 + j \left( \frac{\omega}{\omega_s} \right)} + j\omega\epsilon, \quad (2)$$

where  $\sigma_o$  is the dc conductivity value and  $\omega_s$  is the mean scattering frequency of the charge carrier within the semiconductor given by

$$\omega_s = q/(m^* \mu), \quad (3)$$

where  $q$  is the electronic charge,  $\mu$  is the carrier mobility and  $m^*$  is the effective mass of the charge carrier. The conductivity expression shown in (2) takes into account effects associated with displacement current and charge carrier inertia [3] and will be used in evaluating conductivity within all regions of the device.

An expression for the bulk spreading impedance was first derived by Dickens [4]. In his work, Dickens developed an integral expression for the substrate and skin effect impedance within a cylindrical diode structure by performing a field analysis for potential and current using an oblate spheroidal coordinate system. The integral could not be evaluated analytically, and Dickens introduced two approximations to obtain the following result for the bulk spreading impedance:

$$Z_{\text{sp}} = \frac{1}{2\pi\sigma_{\text{sub}} R_a} \tan^{-1} \left( \frac{R_b}{R_a} \right) + \frac{1 + j}{2\pi\sigma_{\text{sub}} \delta_s} \ln \left( \frac{R_b}{R_a} \right). \quad (4)$$

The first term is referred to as the substrate impedance,  $Z_{\text{sub}}$ , and the second term, the skin effect impedance,  $Z_{\text{skin}}$ . Here the substrate conductivity,  $\sigma_{\text{sub}}$ , is given by the equation analogous to (2). However, in our numerical calculations, we neglected the displacement current term of (2) since the substrate is assumed to be highly doped. The high frequency behavior of  $Z_{\text{sp}}$  is accounted for by this complex conductivity and by the skin effect term,  $\delta_s$ , calculated by

$$\delta_s = \sqrt{\frac{2}{\omega\mu_o\sigma}}, \quad (5)$$

where  $\sigma$  is the dc value of the substrate conductivity.

The first approximation made by Dickens to achieve the result shown in (4), is valid when the radius to the edge of the ohmic contact,  $R_b$ , is much greater than the anode radius,  $R_a$ , a requirement satisfied by most diodes. The

second approximation involves a truncated series expansion of his integral impedance expression to obtain the tractable impedance expression of (4). This integral evaluation has been shown to overestimate real portions of the series impedance by approximately 1  $\Omega$  and reactive portions by 0.5  $\Omega$  at 500 GHz [5]. As a result, this entire analysis of the planar diode series impedance will be confined to 500 GHz in order to remain within tolerable error limits.

## III. DC OHMIC CONTACT IMPEDANCE

This analysis begins by assuming that the ohmic contact region can be modeled as a transmission line [6], as depicted in Fig. 2. With this model it is assumed that:

- (i) the current lines are normal to the equipotential cathode plate,
- (ii) the thickness of the metal and diffusion layers can be neglected,
- (iii) the current-voltage characteristic of the contact is linear.

The sheet resistance under the contact,  $R_s$ , can be estimated as follows:

$$R_s = \frac{1}{q\mu N_{\text{sub}} \min(t_{\text{sub}}, R_b)}. \quad (6)$$

where  $N_{\text{sub}}$  is the substrate doping concentration and  $\mu$  is the carrier mobility. Since the substrate sheet resistance is defined by the dimension with the smallest degree of current bending within the substrate, the smaller of the two dimensions: substrate thickness ( $t_{\text{sub}}$ ) or the inner radius of the ohmic contact ( $R_b$ ), is used to accommodate for this fact. The differential series resistance under the contact is:  $dR = R_s dr/2\pi r$ , while the conductance is:  $dG = 2\pi r dr/\rho_c$ , where  $r$  is the radius of a contact element of width  $dr$  and  $\rho_c$  is the specific contact resistance. As a result, the basic transmission line equations are

$$dV = -I(r) dR \quad (7)$$

$$dI = -V(r) dG \quad (8)$$

where  $V(r)$  and  $I(r)$  represent respectively, the voltage and current distributions in the semiconductor under the equipotential contact at the point  $r$ . These equations can be rearranged to give

$$\frac{d^2 V}{dr^2} + \frac{1}{r} \frac{dV}{dr} - \frac{1}{L_T^2} V = 0, \quad (9)$$

and

$$I(r) = \frac{-2\pi r}{R_s} \frac{dV}{dr}, \quad (10)$$

where

$$L_T = \sqrt{\frac{\rho_c}{R_s}}. \quad (11)$$

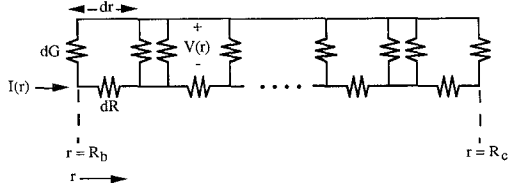


Fig. 2. Radial transmission line model for ohmic contact impedance.

Solution to (9) is of the form:

$$V(r) = AI_o(r/L_T) + BK_o(r/L_T), \quad (12)$$

where  $I_o$  and  $K_o$  represent modified Bessel functions of the first and second kind respectively, and  $A$  and  $B$  are unknown coefficients.

The impedance of the contact is then defined as that encountered between the front edge of the contact and the equipotential metal plate,  $V(R_b)/I(R_b)$ . After imposing the boundary condition that current must be zero at the outer edge of the contact,  $I(R_c) = 0$ , the following expression for  $Z_c$  at dc is obtained:

$$Z_c = \frac{R_s L_T}{-2\pi R_b} \frac{\left\{ I_o \left( \frac{R_b}{L_T} \right) - \frac{I'_o(R_c/L_T)}{K'_o(R_c/L_T)} K_o \left( \frac{R_b}{L_T} \right) \right\}}{\left\{ I'_o \left( \frac{R_b}{L_T} \right) - \frac{I_o(R_c/L_T)}{K'_o(R_c/L_T)} K'_o \left( \frac{R_b}{L_T} \right) \right\}}. \quad (13)$$

The primed terms indicate derivatives with respect to the argument. In the limiting case  $R_b \gg L_T$  and  $R_b \gg R_c - R_b$ , we recover a standard expression for the impedance of a metal strip contact with the length of  $R_c - R_b$  and the width of  $2\pi R_b$  [7]:

$$Z_c = R_s L_T \coth [(R_c - R_b)/L_T]/(2\pi R_b). \quad (14)$$

#### IV. HIGH FREQUENCY OHMIC CONTACT IMPEDANCE

The dc model for ohmic contact impedance developed above is valid for frequencies where the skin depth within the substrate,  $\delta_s$ , is greater than the substrate thickness. For frequencies beyond this limit, an analysis of the current flow in the cylindrical diode configuration, shown in Fig. 3, must be carried out in order to develop an expression for the contact impedance,  $Z_c$ . This begins with Maxwell's curl equations:

$$\nabla \times \mathbf{E} = -j\omega\mu_o \mathbf{H}, \quad (15)$$

and

$$\nabla \times \mathbf{H} = \sigma_{\text{sub}} \mathbf{E}. \quad (16)$$

Here the substrate conductivity,  $\sigma_{\text{sub}}$ , is given by the equation analogous to (2). However, in numerical calculations, we neglected the displacement current which is not important because of a high substrate conductivity. From here, the electric field wave equation is obtained as

$$\nabla^2 \mathbf{E} - j\omega\mu_o \sigma_{\text{sub}} \mathbf{E} = 0. \quad (17)$$

For this axisymmetric problem, only the radial  $E$ -field

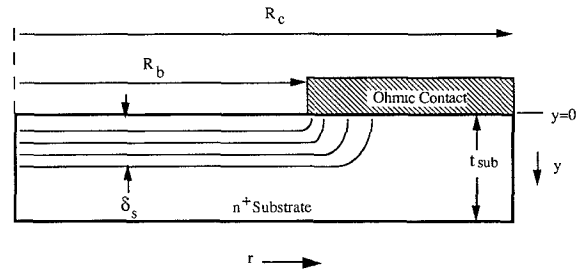


Fig. 3. High frequency current flow in planar diode.

within the substrate will be considered. Furthermore, it is assumed that this  $E$ -field component only has a vertical ( $y$ ) dependence (see axes in Fig. 3.) As a result, (17) can be rewritten as

$$\frac{\partial^2 E_r}{\partial y^2} - j\omega\mu_o \sigma_{\text{sub}} E_r = 0. \quad (18)$$

For this problem, it will be assumed that  $\delta_s \ll t_{\text{sub}}$ , such that the thickness of the substrate can be approximated as being infinite. The following boundary conditions for  $E_r(y)$  can then be imposed:

$$E_r(0) = E_{ro}, \quad (19)$$

and

$$E_r(\infty) = 0. \quad (20)$$

The following solution for  $E_r(y)$  is then obtained:

$$E_r(y) = E_{ro} \exp(-(1+j)y/\delta_s). \quad (21)$$

The current flowing through the substrate is calculated as

$$I = 2\pi r \sigma_{\text{sub}} \int_0^\infty dy E_r(y) \\ = 2\pi r H_{\phi o} = 2\pi r \sigma_{\text{sub}} E_{ro} \delta_s / (1+j). \quad (22)$$

The electric potential can be now introduced in the standard manner from power balance [8]:

$$I dV = 2\pi r P dr, \quad (23)$$

where  $P = -H_{\phi o} E_{ro}$  is the Poynting vector. We should notice that (23) is only valid when the displacement current is small compared to the conduction current. Using  $I = 2\pi r H_{\phi o}$ , we obtain the relationship between the electric field and potential:

$$E_{ro} = -\partial V / \partial r. \quad (24)$$

Under the radial symmetry assumption, the basic transmission line equations can be written as

$$I(r) = \frac{-2\pi r \sigma_{\text{sub}} \delta_s}{1+j} \frac{dV}{dr}, \quad (25)$$

and

$$\frac{dI}{dr} = \frac{-2\pi r V(r)}{\rho_c}. \quad (26)$$

Note that the use of specific contact resistance, a quantity determined at dc, in a high frequency situation is based on the premise that the current-voltage characteristic of the contact at high frequencies is assumed to be the same as that at dc. Using (25) and (26), the differential equation for the voltage distribution beneath the contact is arrived at:

$$\frac{d^2 V}{dr^2} + \frac{1}{r} \frac{dV}{dr} - \frac{V}{L_T^2} = 0 \quad (27)$$

where

$$L_T = \sqrt{\frac{\sigma_{\text{sub}} \delta_s \rho_c}{1 + j}} \quad (28)$$

Note that the electrical transfer length,  $L_T$ , is now a complex quantity. Following the  $Z_c$  formulation of the previous section, the high frequency expression for ohmic contact impedance is obtained:

$$Z_c = \frac{(1 + j)L_T}{-2\pi R_b \sigma_{\text{sub}} \delta_s} \frac{\left\{ I_o \left( \frac{R_b}{L_T} \right) - \frac{I'_o (R_c/L_T)}{K'_o (R_c/L_T)} K_o \left( \frac{R_b}{L_T} \right) \right\}}{\left\{ I'_o \left( \frac{R_b}{L_T} \right) - \frac{I'_o (R_c/L_T)}{K'_o (R_c/L_T)} K'_o \left( \frac{R_b}{L_T} \right) \right\}}. \quad (29)$$

## V. ESTABLISHING THE VALIDITY OF THE LEM

The lumped element model is based on the assumption that current flow radially outward from the anode to the ohmic contact. In the actual planar diode structure, however, the ohmic contact does not extend  $360^\circ$  around the anode (see Fig. 4), and hence, the circumferential components of the current need to be considered if an accurate assessment for series impedance is to be made. Such a numerically intensive analysis can be circumvented by assuming radial current flow from the anode regardless of the angular extent of the ohmic contact. Under this assumption, the series impedance calculated for an axi-symmetric diode can be pro-rated for a given ohmic contact extension angle,  $360^\circ - \theta_s$  (see Fig. 4) to obtain an approximate value for the true series impedance. The pro-rating formula must satisfy two boundary conditions. Obviously, if  $\theta_s$  is  $0^\circ$ , then the impedance value calculated under the axi-symmetric assumption should be obtained. On the other hand, the series impedance should become infinite as  $\theta_s$  approaches  $360^\circ$  (i.e., the ohmic contact is "peeled away.") From this, a first-order asymptotic impedance pro-rating relationship can be written as

$$Z_s = \frac{Z_{\text{cyl}}}{1 - (\theta_s/360^\circ)}, \quad (30)$$

where  $Z_{\text{cyl}}$  represents the series impedance of the cylindrical diode and  $Z_s$  is the impedance of the actual diode structure.

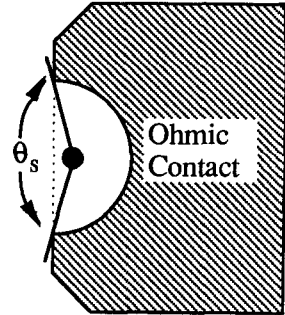


Fig. 4. Top view of actual planar diode geometry.

Under the radial current flow assumption, worst case values for the series impedance are obtained with pro-rating since in reality, current flows along the periphery of the contact, thereby leading to reduction in series resistance. As a result, this contact impedance determination technique can offer a range of series impedance values that can be expected for a given diode design: by using the cylindrical diode impedance as a lower bound and the pro-rated impedance value as an upper bound.

The validity of this method is established upon consideration of Table I, which compares LEM calculated dc series impedance ranges against measured ranges for two diode designs: SC2R4 and SC2T1. The impedance values were pro-rated according to (33), using  $\theta_s = 152^\circ$ , to achieve a range for series impedance. The value for  $\theta_s$  was deduced by noting that for existing designs, the anode is displaced approximately  $2 \mu\text{m}$  from the desired center-point (as shown in Fig. 4) due to ohmic contact encroachment during fabrication.

## VI. ASSESSMENT OF OHMIC CONTACT TECHNOLOGY ON SERIES IMPEDANCE

The LEM predicted ohmic contact contribution to the total diode series impedance is graphed in Fig. 5(a) and (b). These graphs use the SC2R4 diode parameters (see Table I) and are presented for both the dc and 500 GHz cases. Note that in both frequency cases and for all three specific contact resistances, the size of the contact pad can be reduced almost in half without any noticeable increase in the contact resistance. Furthermore, the contribution of the contact impedance at 500 GHz is only slightly higher than that encountered at dc, hence the contact is not expected to degrade electrical performance even at the diode mixing frequency. In addition, these curves establish guidelines regarding the allowable limits for specific contact resistance in small geometry diodes so that device  $I$ - $V$  characteristics are not significantly perturbed as a result of the ohmic contact impedance.

Note that the curves shown in Fig. 5(b) are raised and shifted versions of the curves shown in Fig. 5(a). The shift up in the curves is due to the added inductive component in the contact impedance at operational frequencies. The shift left is a result of the fact that the actual length of the ohmic contact required to support current

TABLE I  
LEM PREDICTED DC SERIES IMPEDANCE RANGE FOR TWO DIODE DESIGNS

Diode Parameter	SC2R4	SC2T1
$R_a$ ( $\mu\text{m}$ )	1.25	0.75
$R_b$ ( $\mu\text{m}$ )	8.00	8.00
$R_c$ ( $\mu\text{m}$ )	100	100
$N_{\text{epi}}$ ( $\text{cm}^{-3}$ )	$2 \times 10^{17}$	$2 \times 10^{17}$
$t_{\text{epi}}$ ( $\mu\text{m}$ )	0.1	0.1
$N_{\text{sub}}$ ( $\text{cm}^{-3}$ )	$2 \times 10^{18}$	$2 \times 10^{18}$
$t_{\text{sub}}$ ( $\mu\text{m}$ )	5.00	5.00
$\rho_c$ ( $\Omega \cdot \text{cm}^2$ )	$2 \times 10^{-5}$	$2 \times 10^{-5}$
LEM calculated dc $Z_s$ range ( $\Omega$ )	4.7–8.1	9.2–15.9
Measured dc $Z_s$ range ( $\Omega$ )	5–7	10–13

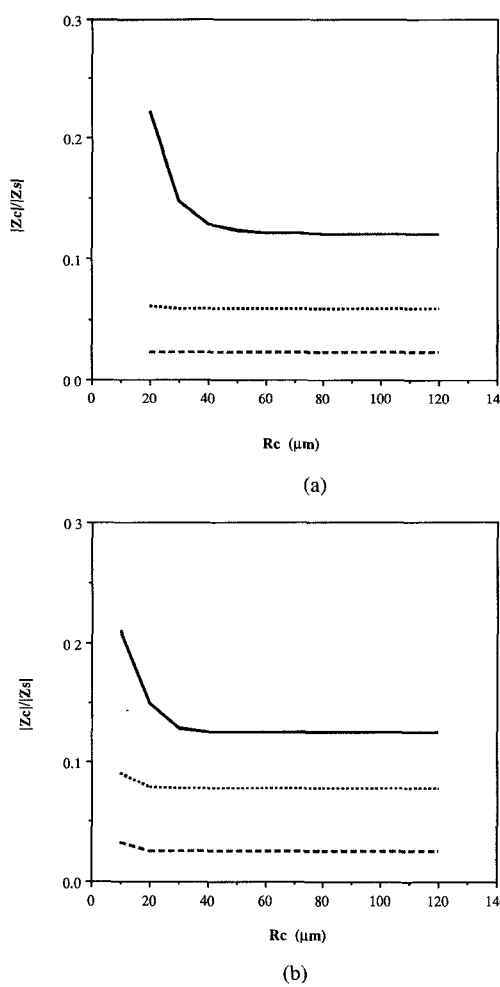


Fig. 5. (a)  $|Z_c|/|Z_s|$  versus  $R_c$  for varying  $\rho_c$  at dc. (b)  $|Z_c|/|Z_s|$  versus  $R_c$  for varying  $\rho_c$  at 500 GHz.

flow at high frequencies is reduced from its DC value. This relationship between the magnitude of the electrical transfer length,  $|L_T|$ , and frequency, is shown in Fig. 6.

## VII. SUMMARY

An assessment of the impact of ohmic contact technology on the electrical characteristics of GaAs planar Schottky diodes has been made using a lumped element model (LEM) for series impedance components. The

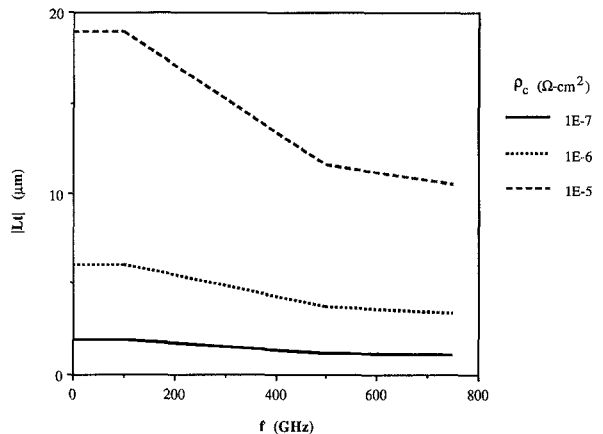


Fig. 6.  $|L_T|$  versus frequency for different ohmic contacts.

LEM divides the series impedance into three parts: epilayer impedance, bulk spreading impedance and ohmic contact impedance. Expressions for the first two components were derived by other researchers and used in this investigation. An expression for ohmic contact impedance was formulated using a transmission line model that accurately portrays the role of specific contact resistance on the measured contact resistance. The accuracy of the LEM is frequency limited to about 500 GHz due to errors introduced by the spreading impedance expression. One important note, the LEM was developed for a axi-symmetric diode. However, a range for series impedance can be calculated by pro-rating the impedance value calculated under this assumption.

This pro-rating technique was shown to be accurate when comparing the LEM with measured values for dc series impedance. In characterizing the ohmic contact impedance, it was found that its contribution was small in comparison to that of the other components, both at dc and at operational frequencies. This means that the dimensions of the contact pad can be scaled down significantly without any increase in series impedance but with a decrease in the parasitic pad-to-pad capacitance. Hence, diodes that have smaller contacts pads are expected to have higher cutoff frequencies; enabling their use in space-based and other high-frequency applications.

## REFERENCES

- [1] T. Newman and K. T. Ng, "A submillimeter-wave planar diode mixer—design and evaluation," in 1991 IEEE MTT-S Microwave Symp. Dig., Boston, pp. 1293–1296.
- [2] G. K. Reeves, "Specific Contact Resistance using a Circular Transmission Line Model," *Solid-State Electron.*, vol. 23, pp. 487–490, 1980.
- [3] K. S. Champlin, D. E. Armstrong, and P. D. Gunderson, "Charge carrier inertia in semiconductors," *Proc. IEEE*, vol. 52, pp. 677–685, June 1964.
- [4] L. E. Dickens, "Spreading Resistance as a Function of Frequency," *IEEE Trans. Microwave Theory Tech.*, vol. MTT-15, no. 2, pp. 101–109, Feb. 1967.
- [5] U. Bhapkar, "An investigation of the series impedance of GaAs Schottky barrier diodes," M.S. thesis, University of Virginia, May 1990, p. 37, unpublished.
- [6] W. Shockley, AF Avionics Lab Tech. Rep. No. AL TDR 64-207, Wright Patterson Air Force Base, Ohio, 1964, Appendix B.

- [7] M. Shur, *Physics of Semiconductor Devices*. Englewood Cliffs, NJ: Prentice-Hall, 1990.
- [8] L. D. Landau and E. M. Lifshitz, *Electrodynamics of Continuous Media*. London: Pergamon, 1960.



**Kaushik Bhaumik** received the B.S.E.E. (with distinction) and M.S.E.E. degrees in May of 1991 from the University of Virginia, Charlottesville.

During the summer of 1990, he worked on ECL circuit design and characterization at Cray Research, Chippewa Falls, WI. He is currently pursuing the Ph.D. degree in electrical engineering at Cornell University, Ithaca, NY. His doctoral work concerns the analysis and design of Group IV heterostructure field effect transistors. His research interests include heterostructure device physics, process development and related device integration issues.

Mr. Bhaumik is a member of Tau Beta Pi and Eta Kappa Nu.



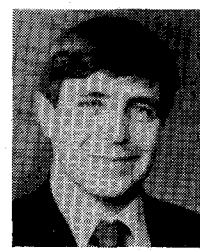
**Boris Gelmont** received the M.S.E.E. degree from Leningrad Electrotechnical Institute in 1960, the Ph.D. degree in physics from A. F. Ioffe Institute of Physics and Technology in 1965 and Doctor of Science degree (Habilitation) from Ioffe Institute in 1975.

Since 1960, he has been with A.F. Ioffe Institute where he is now a Leading Scientist. He is also a Professor at the Politechnical Institute in Leningrad. In 1982, he was awarded a State Prize (for the theory of gapless semiconductors). Since 1990, Dr. Gelmont has also been a Visiting Professor and Senior Scientist in the Department of Electrical Engineering of the University of Virginia in Charlottesville.

Dr. Gelmont has published more than 150 technical papers in refereed journals, several book chapters and reviews. He received two patents on solid-state devices and presented more than 50 invited and contributed talks

at international and national conferences. His research includes narrow-gap semiconductors, semimagnetic semiconductors, vitreous semiconductors, disordered systems, solid state plasma, recombination processes, spectroscopy of impurities, semiconductor devices.

**Robert J. Mattauch** (S'61-M'66-SM'81-F'86), for a photograph and biography, see this issue, p. 819.



**Michael Shur** (M'78-SM'80-F'89) received his M.S.E.E. degree (with honors) from St. Petersburg Electrotechnical Institute in 1965 and Ph.D. in Physics from A.F.Ioffe Institute of Physics and Technology in 1967.

From 1965 to 1976 he was with A.F.Ioffe Institute of Physics and Technology. In 1976 he joined the Department of Electrical Engineering of Wayne State University, Detroit, MI. In 1978 he was with the School of Engineering of Oakland University, Rochester, MI. In 1976-1980 he had visiting summer appointments with the School of Electrical Engineering of Cornell University. In the summer of 1979 he was a visiting faculty at IBM T. J. Watson Research Center. From 1979 to 1989 he was with the University of Minnesota. Since 1989, he is John Marshall Money Professor of Electrical Engineering at the University of Virginia. His research has included ferroelectrics, amorphous semiconductors, solar cells, ballistic transport, high speed semiconductor devices, and integrated circuits. He published several books, including a book on GaAs devices published by Plenum in 1987 and a book on physics of semiconductor devices (with microcomputer programs) published by Prentice Hall in 1990.

Dr. Shur is a member of American Physical Society, a member and a Vice Chairman of the National Chapter of Commission D of International Union of Radio Science, a member of Electromagnetic Academy, a member of the Editorial Board of *International Journal of High Speed Electronics*, Eta Kappa Nu, and an Associate Editor of *IEEE TRANSACTIONS ON ELECTRON DEVICES*.